Direct hole and delayed electron capture on a picosecond timescale by Eu^{2+} centers in $CaGa_2S_4$ monitored by synchroscan with horizontal blanking

D. J. Louwers,[1] T. Takizawa,[2] C. Hidaka,[2] and E. van der Kolk[1]
[1]*Delft University of Technology, Luminescent Material Research Group, Mekelweg 15, 2629JB Delft, The Netherlands*
[2]*Nihon University, 3-25-40 Sakurajosui, Setagaya-ku, Tokyo, Japan*

(Received 13 December 2011; accepted 2 April 2012; published online 4 May 2012)

A Eu^{2+} concentration and temperature dependent energy transfer study from the host lattice to Eu^{2+} luminescence centers in $Ca_{(1-x)}Eu_xGa_2S_4$ ($x = 0.001$ to 0.05) was performed with a special streak camera that combines the high timing resolution of a conventional synchroscan operation (<2 ps) with the ability to study long lived states (10 ns – 1 ms) typical for rare earth and transition metal ions. Two transfer mechanisms from the $CaGa_2S_4$ host lattice to the Eu^{2+} ions were identified. A fast transfer process (<4 ps) is interpreted as sequential hole-electron capture by the Eu^{2+} ions, and slower process (>1 ns) is interpreted as the sequential capture of a hole and an electron by Eu^{2+} but with the electron first entering an intermediate state trapped near Eu^{3+}. Energy transfer via a self-trapped excitonic (STE) state is unlikely because of the absence of an anti-correlation between the STE decay-time and the Eu^{2+} rise-time as well as between the STE emission intensity and the Eu^{2+} intensity. All rise-time spectra were successfully fitted with a model representing the above transfer mechanisms. © *2012 American Institute of Physics*. [http://dx.doi.org/10.1063/1.4709757]

I. INTRODUCTION

Knowledge on energy transfer to luminescence centers like transition metal (TM) and rare earth (RE) ions in doped insulators and semi-conductors after bandgap excitation is of importance for development and understanding of new Electroluminescent Displays (ELDs), light-emitting diodes (LEDs), radiation detector materials but also for improving photo-voltaic devices. For the latter, spectral conversion materials or materials for luminescent solar concentrators are needed in the form of thin-films that strongly absorb ultra-violet and visible sunlight in the band-gap and have efficient near infrared RE or TM-ion emission. In most materials, however, RE or TM luminescence efficiencies are low upon bandgap excitation because of the many possible alternative relaxation routes like charge trapping or the formation of excitonic species with subsequent radiative or non-radiative relaxation. Deeper insight in these picosecond timescale processes and how they are related to composition, structure, and the impurity ion energies relative to the valence and conduction band can be obtained from decay-time spectra on a nanosecond timescale.[3,4] However, more direct information on host-to-luminescence center transfer can be obtained by studying luminescence rise-time profiles. Rise-time studies on such short timescale have been reported for undoped materials like the alkali halides in which the formation of self-trapped excitons (STEs) is a dominant process.[1–3] Although Moses and Weber[5,6] studied rise-times in wide bandgap Ce^{3+} doped scintillator materials under pulsed x-ray excitation, host-to-luminescence center rise-time studies using selective laser excitation at bandgap energies on TM or RE ion doped materials have hardly been reported.

In this work, we present a special streak camera that combines the high timing resolution capabilities of synchroscan (<2 ps) with the ability of measuring long lived states (μs-ms) typical for RE and TM ions. This is accomplished by a custom made horizontal blanking unit that is incorporated in a normal synchroscan streak camera. We report on the Eu^{2+} emission rise-times measured upon excitation in the $CaGa_2S_4$ host lattice. $CaGa_2S_4$ is a small bandgap material that when doped with Eu^{2+} or Ce^{3+} is considered for application in ELD and LED devices. This paper is organized as follows. In the experimental section, we first discuss the laser excitation and streak camera detection setup, including the horizontal blanking unit and briefly describe applied techniques such as streak camera gating and sequenced recording. Then we present the time resolved luminescence spectra, both as a function of Eu^{2+} concentration and temperature. Thereafter, a model is presented describing the observed rise- and decay-times and fit the model to our time resolved data. In the discussion section, it will be explained that hole trapping by Eu^{2+} is the dominant transfer mechanisms followed by prompt or delayed electron trapping. Also the role of STEs will be discussed.

II. EXPERIMENTAL METHODS

$CaGa_2S_4$ powders doped with Eu^{2+} concentrations ranging from 0.1 mol. % to 5.0 mol. % were prepared by solid state reaction between CaS, Ga_2S_3, and EuS in powder form. The starting materials were weighed to 0.5 g in total in an Argon atmosphere, sealed under vacuum (10^{-4} Pa), and then sintered at 1135 °C for 1 h as described earlier in more detail in Ref. 7. The excitation and emission spectra shown in Figs. 2 and 3 were recorded using a closed cycle helium refrigerator connected to a photo-luminescence excitation and emission facility that was described in Ref. 8. Temperature

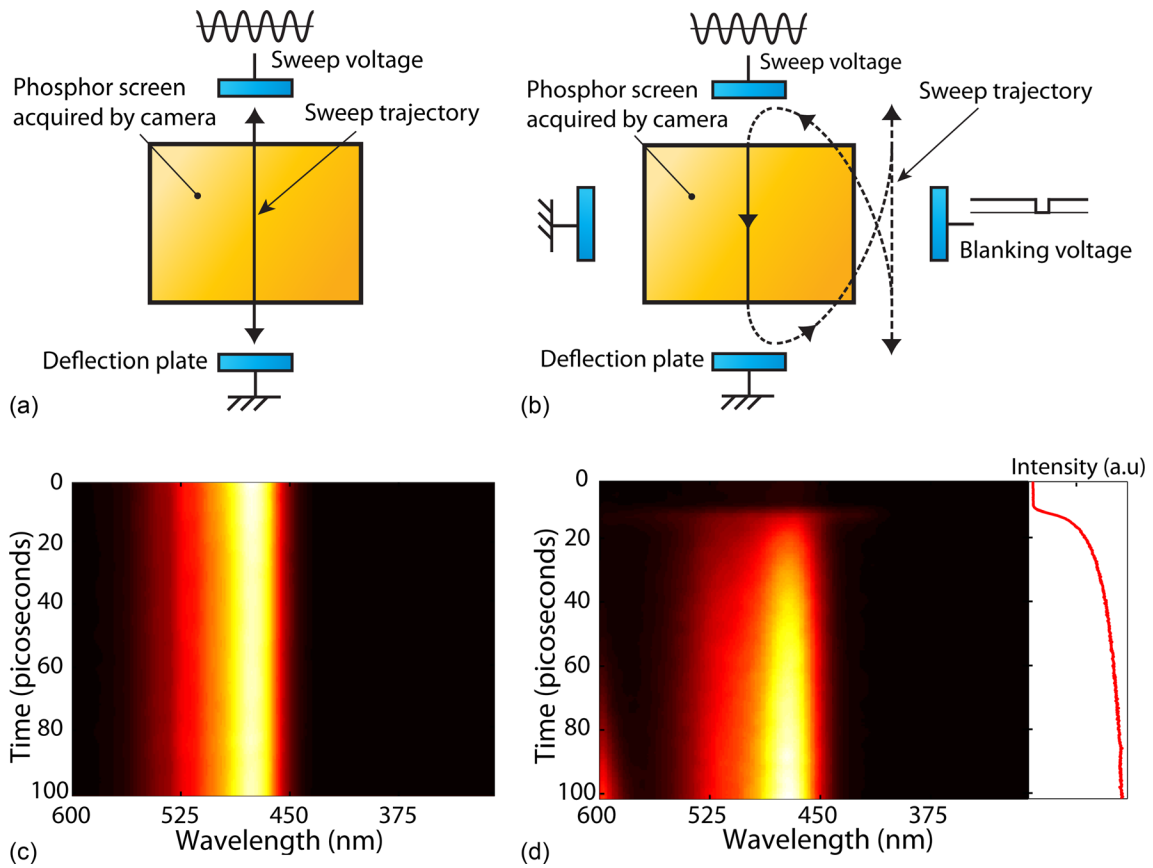

FIG. 1. (a) Schematic representation of normal sysnchroscan mode, with corresponding streak image (c) of a $CaGa_2S_4:Ce^{3+}$ sample. (b) Schematic representation of horizontal blanking with (d) the corresponding streak image of the same sample. The samples were excited with 250 nm laser pulses at 10 kHz.

dependent streak camera measurements were recorded with the powder attached to a copper cold finger of a liquid nitrogen cryostat as described in Ref. 9.

A mode-locked $Ti:Al_2O_3$ laser system (Coherent, Inc., model Mira 900F, pumped by a 10 W Coherent, Inc., Verdi V-10 laser) provided femtosecond pulses (~120 fs FWHM) with a repetition rate of 76 MHz. To accomplish shorter pulse separation times, a pulse picker was employed (APE Pulseselect) which is synchronized with the fast internal photodiode output of the Mira and is externally triggered with a 10 kHz signal derived from the internal Mira photo-diode. To reach about 4 eV bandgap energy of $CaGa_2S_4$, a third harmonic generator was used (Photop TP-2000B). All the measurements reported in this work were carried out at a 250 nm (5 eV) excitation energy.

Luminescence was imaged into a Czerny-Turner type spectrograph (Acton research SP2300) and projected through the entrance slit of a streak camera (Hamamatsu 5680). The 10 ns timescale measurements (Fig. 4) were

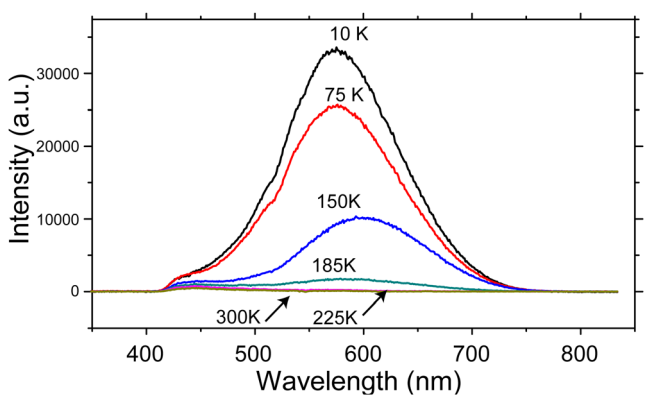

FIG. 2. Emission spectra of undoped $CaGa_2S_4$ sample excited at 250 nm at different temperatures.

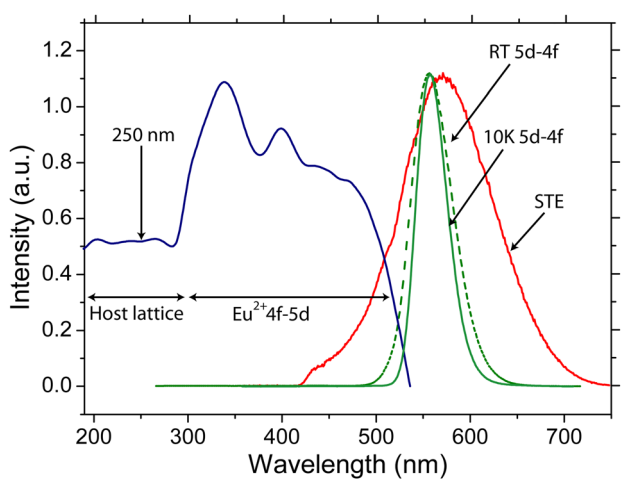

FIG. 3. Excitation spectrum (left blue curve) monitoring 550 nm of $CaGa_2S_4$: 1.5% Eu^{2+} at room temperature and emission spectra recorded 10 K (solid green curve) and room temperature (dashed green curve). The 10 K emission spectrum of undoped $CaGa_2S_4$ is shown for comparison (red curve). All emission spectra were recorded under 250 nm excitation.

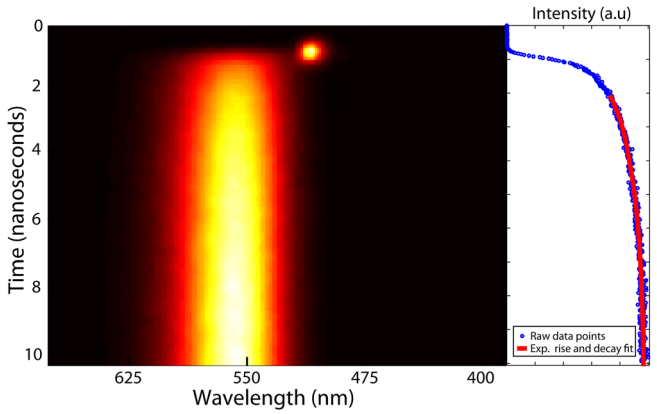

FIG. 4. Streak image of 1.5 mol% Eu^{2+} doped $CaGa_2S_4$ at 10 ns time scale at room temperature (single sweep mode). Excitation was at 10 kHz with 250 nm laser pulses. The second order diffracted laser spot is visible at 500 nm.

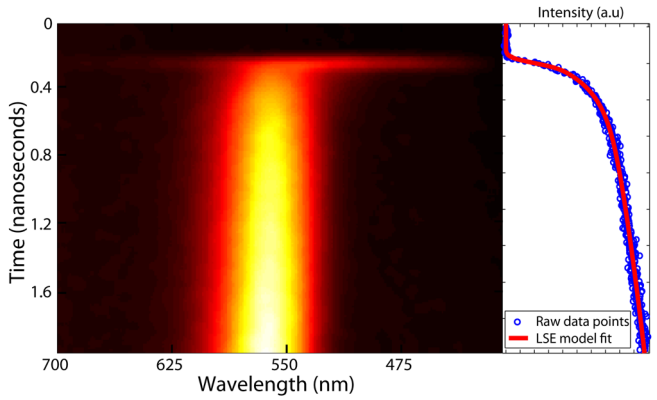

FIG. 5. Streak image of 1.5 mol. % Eu^{2+} doped $CaGa_2S_4$ at 2 ns time scale at room temperature (synchroscan mode, 48 ps IRF FWHM). Excitation was at 10 kHz with 250 nm laser pulses. The solid red curve in the right panel is a fit by the model presented in the analysis of the results section.

recorded with the streak camera in single sweep mode, using a Hamamatsu 5677 streak unit that roughly has a FWHM instrument response function (IRF) of 2% of the timescale. All other measurements (Figs. 5–8) were acquired in synchroscan mode (Hamamatsu 5675). This means that the vertical sweep electrodes are phase-locked with the fundamental frequency of the laser (76 MHz) by a fast photodiode (Hamamatsu C1808) that is used as a vertical sweep input signal. The trigger timing and phase-locking in synchroscan mode are controlled by a Hamamatsu C6878 delay generator.

Figs. 1(a)–1(d) compare normal synchroscan operation (1(a) and 1(c)) and synchroscan with horizontal blanking (1(b) and 1(d)). In the latter case, the electron beam is horizontally deflected of the screen after a single vertical sweep in order to prevent detection of luminescence in the next vertical sweep. Besides blanking, a technique called gating needed to be applied. Gating renders the streak camera temporarily insensitive. This drastically reduces the noise caused by thermal electrons which are multiplied inside the streak tube in the relatively long electron beam blanking interval.

Measuring at lower repetition rates (typically 10 kHz) obviously introduces longer acquisition times. In addition when only the first 100 ps after excitation are considered of materials with large lifetime constants, a very small percentage of emitted photons is actually detected. It is therefore not surprising that our streak image acquisition times are in the order of tens of hours instead of seconds which is more common for normal synchroscan measurements.[10] One of the encountered problems with such long acquisition times is the long-term drift of the phase-locked vertical sweep trigger delay. This drift causes an increase in the intrinsic 2 ps synchroscan time resolution. By using sequenced recording, a measurement is divided in individual sequences of typically several minutes and by detection of reflected laser light, one can generate a timestamp to merge the individual sequences back together with a relative vertical offset correction. Sequenced recording allows for a time resolution of typically 3–5 ps independent on the acquisition time.

III. EXPERIMENTAL RESULTS

A. Luminescence excitation and emission

The emission spectra of an undoped $CaGa_2S_4$ sample are presented as a function of temperature ranging from 10 K (black curve) to 300 K (brown curve) in Fig. 2. Broad band emission is observed at 250 nm bandgap excitation that is centered around 560 nm and is interpreted as self-trapped exciton emission. Fig. 2 shows that the STE emission quenches rapidly towards higher temperature and has practically zero intensity at 200 K and above. A small shift of the emission maximum toward longer wavelengths is observed for which we have no clear explanation. In Fig. 3, the

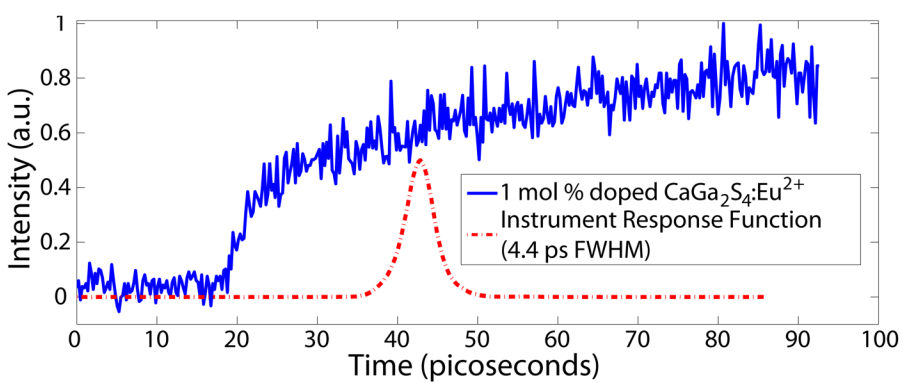

FIG. 6. Spectrally integrated time resolved measurement of 1 mol. % Eu^{2+} doped $CaGa_2S_4$, excited at 10 kHz with 250 nm pulses at room temperature.

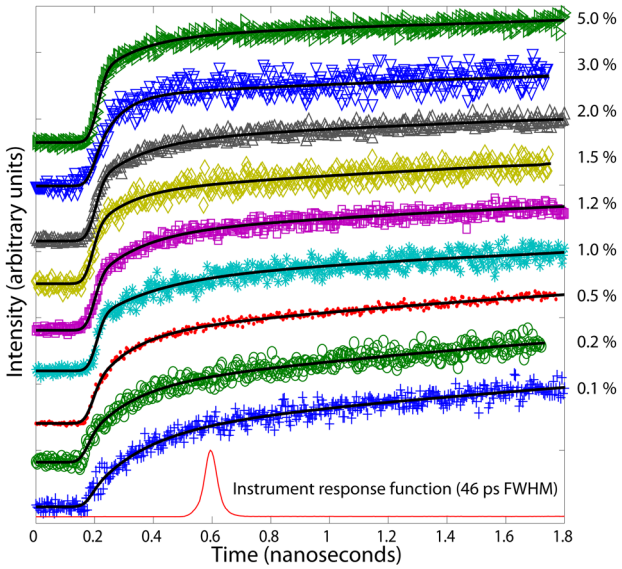

FIG. 7. Spectrally integrated time resolved streak image data of $CaGa_2S_4$ doped with different Eu^{2+} concentrations excited with 250 nm fs pulses at room temperature. The drawn curves are fits by the model presented in the analysis of the results section.

emission spectra of an undoped and a Eu doped sample are compared under identical temperature (10 K) and excitation wavelength (250 nm) conditions. Clearly, all STE emission that is present in the undoped sample is completely quenched upon Eu^{2+} doping in favor of Eu^{2+} 5d → 4f emission. Apparently under bandgap excitation, energy is transferred efficiently to the Eu^{2+} ions. This is in accordance with the non-zero intensity at 250 nm observed in the RT excitation spectrum of $CaGa_2S_4$:Eu^{2+} monitoring Eu^{2+} d → f emission at 550 nm that is also presented in Fig. 3. The excitation spectrum consists of 4f→5d excitation bands between 300 and 500 nm. The decrease in intensity around 300 nm (~4 eV) is caused by $CaGa_2S_4$ host lattice absorption. This bandgap value corresponds well with published absorption data.[7] The RT emission spectrum consists of a single broad band (55 nm FWHM) centered around 560 nm which is typical for Eu^{2+} 5d→4f emission. Both 5d emission and excitation bands are in accordance with earlier observations by, for example, Takizawa[7] or Bessiere.[11]

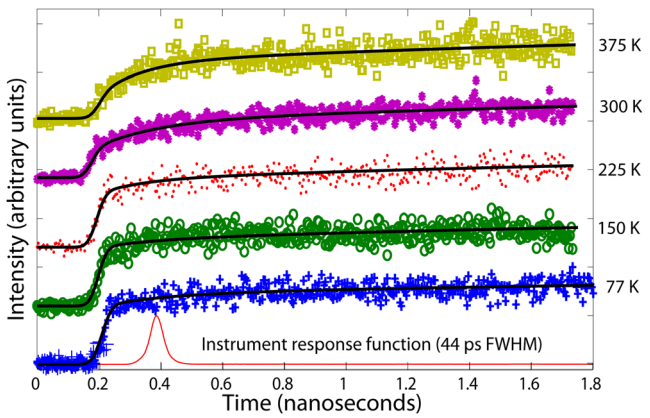

FIG. 8. Spectrally integrated temperature dependent time resolved Eu^{2+} emission of 1.2 mol. % doped $CaGa_2S_4$ excited with 250 nm fs pulses. The drawn curves are fits by the model presented in the analysis of the results section.

B. Concentration and temperature dependent rise-time

Nine different $CaGa_2S_4$ powder samples with Eu^{2+} doping concentrations ranging from 0.1 to 5 mol. % were used to measure the concentration dependent rise- and decay-time characteristics of the Eu^{2+} emission. A measurement on a 10 ns timescale is shown in Fig. 4. Some reflected laser light, visible in second order at 500 nm can also be seen. With an IRF of 190 ps, a rising component in the emission on a ns timescale can clearly be observed and is indicated by the solid red curve in the right panel. A measurement on a 2 ns time interval shown in Fig. 5 shows weak broad band emission with a decay-time of several tens of ps. This emission is at the same wavelength as the STE emission shown in Fig. 2 of the undoped sample. It is therefore interpreted as strongly quenched STE emission. It is important to note that the STE decay-time is much shorter than the observed slow rise-time component of Eu^{2+} emission which is in the order of ns. Both the decay-time of the STE and the steep slope of the rise in the Eu^{2+} emission that is plotted in the right panel of Fig. 5 are equal to the 45 ps IRF measured on this timescale. The right panel of Figs. 4 and 5 also includes fits (red solid curve) by a model that will be presented later.

Fig. 6 represents the spectrally integrated time resolved emission of a 1 mol. % Eu^{2+} doped $CaGa_2S_4$ sample on a timescale of 100 ps. This measurement has an IRF of 4.4 ps and shows that there is still a fast emission rise-time component shorter than the IRF.

In Fig. 7, all spectrally integrated time resolved Eu^{2+} emission spectra for different Eu^{2+} concentrations are plotted together. This data was acquired in the same way as the data presented in Fig. 5. The drawn lines are again fits by a model that will be described later. The measured IRF is also plotted in red at the bottom of the figure. Although a detailed analysis of the spectra will follow in the analysis of the results section, we can already give a qualitative description of the trends. First of all, a clear fast rise (called component 1) after excitation in the first ~100 ps can be seen which presence becomes less clear toward lower Eu^{2+} concentration. Second after the fast rise, a slower rise (called component 3) in intensity can be observed that takes place on a timescale of nanoseconds. After about 2 ns, this rise is seen on this timescale as a line that is approximately straight. The slope of this line becomes steeper at lower Eu^{2+} concentration. The shortest timescale measurements (Fig. 6) reveal a second rise-time component (component 2) dominating before 2 ns.

In Fig. 8, all spectrally integrated time resolved spectra of $CaGa_2S_4$ doped with 1.2 mol. % Eu^{2+} at 5 different temperatures ranging from 77 K to 375 K are plotted together. The drawn lines are again fits by a model that is further described in the analysis of the results section. The measured IRF is also plotted in red at the bottom of the figure. The same three rise components 1, 2, and 3 as described for the concentration dependence can be observed. The fastest component becomes less visible towards higher temperature. The

slope of the slowest component becomes steeper towards higher temperature.

IV. ANALYSIS OF THE RESULTS

A. Fitted model

For almost all doping concentrations and temperatures, there is a fast energy transfer component 1, together with two slower components 2 and 3. This can be explained as follows. First, free excitons are created (state A) which can either transfer their energy via direct hole-electron capture to Eu^{2+} resulting in excited Eu^{2+} ions (state D). Transfer can also proceed via intermediate states (B and C). These intermediate states "slowly" transfer their energy to Eu^{2+} (state D) that finally emits reaching the ground state of Eu^{2+} (state E).

The direct transfer from A to D corresponding to process 1 appeared faster than our measurement capabilities (<4 ps). Therefore, we can model this as an "instant" transfer giving excited Eu^{2+} ions at t = 0 and thus a straightforward single exponential decay intensity profile for Eu^{2+} emission.

As will be motivated in the discussion section, the transfer from state A to state B is assumed to take place on the same timescale as the transfer from A directly to state D (they both involve hole trapping at Eu^{2+}). This transfer can, therefore, be described by omitting the step from A to B as it is too fast to detect. The time resolved intensity due to transfer via state B is found by solving the rate equations for this system and is given by

$$\Gamma_{DE} D(t) = \frac{\Gamma_{DE}\Gamma_{BD}}{\Gamma_{BD} - \Gamma_{DE}} (e^{-\Gamma_{DE}t} - e^{-\Gamma_{BD}t}). \quad (1)$$

A similar formula holds for transfer via state C. It is assumed that the three transfer processes are independent so that the measured time resolved intensity profile is a summation of three terms,

$$I(t) = f_1 \Gamma_{DE} e^{-\Gamma DE t} + f_2 \frac{\Gamma_{DE}\Gamma_{BD}(e^{-\Gamma_{DE}t} - e^{-\Gamma_{BD}t})}{\Gamma_{BD} - \Gamma_{DE}} + f_3 \frac{\Gamma_{DE}\Gamma_{CD}(e^{-\Gamma_{DE}t} - e^{-\Gamma_{CD}t})}{\Gamma_{CD}\Gamma_{DE}}, \quad (2)$$

with $f_1 + f_2 + f_3 = 1$ and f_i being the fraction of the total amount of photons emitted due to transfer via respective process 1, 2, or 3. The actual measured response is a convolution of Eq. (2) with the Gaussian shaped measured IRF $h(t)$ shown in, for example, Figs. 7 and 8

$$R(t) = I(t) * h(t) = \int_{-\infty}^{\infty} I(t) \cdot h(t) dt. \quad (3)$$

$R(t)$ has finally been used to acquire the fitting parameters f_1, f_2, f_3, $\tau_d (= \frac{1}{\Gamma_{DE}})$, $\tau_C (= \frac{1}{\Gamma_{CD}})$, and $\tau_b (= \frac{1}{\Gamma_{BD}})$ by fitting $R(t)$ to the measured data shown in Figs. 7 and 8.

B. Fitting procedure and fitting parameters

First, the Eu^{2+} decay constant τ_d is fitted with a single exponential decay using data recorded on a 5 μs timescale (not shown). A value of τ_d = 660 ns was fitted and found to be approximately constant for all Eu^{2+} concentrations and temperatures. Up to 5 mol. % and 350 K, no significant Eu^{2+} luminescence quenching is observed. Next, the rise-time τ_c was obtained by fitting formula (1) to the data plotted in Fig. 4, keeping τ_d fixed at the value determined in the first fitting step. By omitting the first 2 ns from the data, as shown by the solid red curve in the right panel of Fig. 4, the fast rise component 1 and component 2 (τ_b) are omitted so that the fitted rise-time can be appointed to component 3 only. Finally, the fitting parameters f_1, f_2 and f_3, and τ_b were derived from the data presented in Figs. 7 and 8 by fitting with formula (3). τ_c and τ_d were kept fixed in this final fitting step at values that were determined in the first two fitting steps described above.

The trends of fitting parameters as a function of temperature and Eu^{2+} concentration that were already noted qualitatively in the result section can now be confirmed and made quantitative in Fig. 9 using the results of the fitting procedure described above. The error bars represent the 95% confidence intervals for the least square estimated fitting parameters of the model. Indeed fraction f_1 representing the fast rise (process 1) becomes smaller towards lower Eu^{2+} concentration. It drops from 0.5 to 0.1 when the Eu^{2+} content drops from 5 to 0.1 mol. % as can be seen by the blue circles in Fig. 9(b). This drop in f_1 is compensated by an increase of f_3 while f_2 remains practically constant. Also the observation that the slope of slow rise-time component (process 3) becomes steeper with lower Eu^{2+} content is confirmed because the rise-time constant τ_c increases from 2.2 to 3.3 ns when the Eu^{2+} concentration drops from 5 to 0.1 mol. %, as can be seen by the square symbols in Fig. 9(a). No significant change of τ_b was observed. In the result section, it was noted

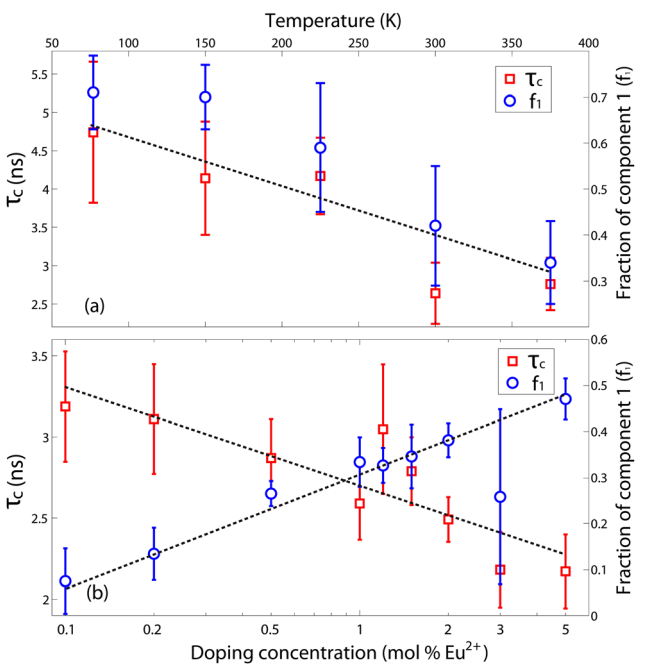

FIG. 9. Fitted parameters f_1 and τ_c versus temperature (a) and Eu^{2+} doping concentration (b). The error bars represent the 95% confidence intervals for the least square estimated fitting parameters of the model (Eq. (3)). The dashed lines serve as a guide to the eye.

that the fastest component 1 becomes less visible towards higher temperature. This is clearly confirmed by Fig. 9(a) (blue circles) showing that f_1 drops from 0.7 to 0.3 as the temperature increases from 77 to 375 K. This drop in f_1 is compensated by an increase of f_3 while f_2 remains practically constant. The observed steepening towards higher temperature of the slope of the slowest rise-time component 3 is also confirmed. The rise-time constant τ_c decreases from 5.0 to 2.5 ns as the temperature increases from 77 to 375 K, as can be seen in Fig. 9(a).

V. DISCUSSION

It was observed that, in the absence of Eu^{2+} ions, electrons and holes relax to form STE states that emit around 560 nm at low temperature. As soon as Eu^{2+} is doped in $CaGa_2S_4$ however, STE emission is quenched almost completely even at 0.1% Eu^{2+} doping. This was concluded from the absence of STE emission in Fig. 3. This can be explained by assuming that STEs are hardly formed in Eu^{2+} doped $CaGa_2S_4$ because the capture of a hole by Eu^{2+} is energetically more favorable than V_k-center formation. The Dorenbos energy level scheme for $CaGa_2S_4$:Ln^{2+}/Ln^{3+}(Ref. 11) shows that hole trapping by Eu^{2+} releases as much as 2 eV which is energetically more favorable forming a V_k-center. This can explain the quenching of the STE emission by Eu^{2+} doping.

Our time resolved data reveal two different relaxation routes leading eventually to excitation of Eu^{2+} and the typical d→f emission. The first route of exciton-to-Eu^{2+} transfer (process 1) takes place on a timescale shorter than 4 ps, which is the limit of the time resolution of our detection system. As hole trapping is often observed as a picosecond timescale process,[3,4] the observed fast rise-time present in all our time resolved spectra may therefore be explained by direct capture of a hole by Eu^{2+} followed by the capture of an electron by Eu^{3+} leaving Eu^{2+} in the excited 5d state. This sequential hole-electron capture has been observed before in Ce^{3+} doped scintillator studies.[1,2] The efficiency of STE quenching at very low Eu^{2+} (0.1%) doping levels suggests that holes are free to migrate after photo-excitation. Apparently photo-excitation at 250 nm does not involve a resonant excitation of a bound exciton. This is in accordance with the flat and structureless shape of the excitation spectrum shown in Fig. 3. Still a clear increase in the exciton-to-Eu^{2+} transfer efficiency is observed with increasing doping concentration by a factor of 50 from 0.1 mol. % to 5 mol. % Eu^{2+}. This may be explained by a concentration dependent electron transport to Eu^{3+}.

A second route of exciton-to-Eu^{2+} transfer takes place on a longer timescale as can be seen from the rise-times detected in our streak images of which cross-sections are shown in Figs. 7 and 8. An increase in energy transfer via these slower processes was observed with increasing temperature (Fig. 9(a)). The observed rise-times suggest that these slower transfer processes 2 and 3 correspond to intermediate precursor states between the moment of excitation and the formation of excited Eu^{2+} ions that have a lifetime of 200 ps (component 2) and 3 ns (component 3), respectively. The observed decrease in lifetime with increasing temperature suggests that some thermal energy is required to further transfer the energy to Eu^{2+}.

One can consider two possible descriptions of the nature of these short lived states. The first possibility may involve fast (prompt) hole capture by Eu^{2+} but with an electron trapped nearby in a shallow trap that requires thermal stimulation to recombine with Eu^{3+}. The second may be the formation of a STE that requires some thermal stimulation to recombine further at a neighboring Eu^{2+} center. Both models can explain the observed (Fig. 9(a)) temperature dependent rise-time τ_c.

It was already concluded that STE emission was quenched upon Eu^{2+} doping. However if the transfer from the STE to Eu takes place on a sub ns timescale, the intensity is expected to be low, possibly below the noise level of the emission spectra shown in Fig. 3. If there would be any energy transfer via a STE, the observed rise-time of Eu^{2+} emission (0.2–3 ns) should be the same as the decay-time of the STE emission. The faint, short lived, broad band emission observed at room temperature (Fig. 5) was ascribed to STE emission. Clearly, the decay-time of the STE emission appears which is not related to the slow rise-time component of the Eu^{2+} luminescence. Another argument against transfer via STE formation is the strong quenching of the STE emission with temperature which is not accompanied with a corresponding increase in the Eu^{2+} 5d-4f emission. Furthermore STE temperature quenching should result in an identical temperature dependent rise-time of Eu^{2+} emission. As seen in Fig. 9(a), there is a temperature dependent rise-time of component 3, but not in the order of magnitude of what is expected when considering the temperature quenching of the STE emission in Fig. 1. These three arguments make the possibility of any significant energy transfer via a STE unlikely.

Our experimental data can, in our opinion best, be explained by assuming that the precursor states represent an electron in a shallow trap. Shallow electron traps in the $CaGa_2S_4$ lattice have been observed by low temperature thermo-luminescence measurements[12] and can explain the temperature dependent electron transfer to the Eu^{3+} ions. It may be that the hole self-trapping at Eu^{2+} induces electrons to become localized in Ga-s orbitals[13] that are nearest neighbor to the trapped hole. The capture of this trapped electron may require a small amount of thermal stimulation.

VI. CONCLUSION

We have successfully built a measurement setup with the unique ability of monitoring very short rise-times of long decay curves. The setup consists of a femtosecond laser with a streak camera with a custom made horizontal blanking unit that, with the help of streak camera gating and sequenced recording techniques, result in an instrument response function of 4 ps (FWHM).

At least two different ways of energy transfer from the $CaGa_2S_4$ host lattice to Eu^{2+} ions were identified. A fast (<4 ps) rise-time component is identified as direct hole-electron capture by Eu^{2+}. The observed nanosecond timescale rise-time is interpreted as direct hole capture by Eu^{2+}

ions, followed by delayed electron transfer via shallow electron traps.

ACKNOWLEDGMENTS

This work is part of the Joint Solar Programme (JSP) of the Stichting voor Fundamenteel Onderzoek der Materie (FOM) and financially supported by Nuon Helianthos. We thank Pieter Dorenbos for carefully reading the manuscript.

[1]G. Bizarri and P. Dorenbos, Phys. Rev. B **75**, 184302 (2007).
[2]G. A. Bizarri and P. Dorenbos, J. Phys.: Condens. Matter **21**, 235605 (2009).
[3]K. S. Song and R. T. Williams, *Self-Trapped Excitons* (Springer-Verlag, Berlin, 1993).
[4]M. Ueta, *Excitonic Processes in Solids* (Springer-Verlag, Berlin, 1986).
[5]M. J. Weber, S. E. Derenzo, and W. W. Moses, J. Lumin. **87–89**, 830 (2000).
[6]S. E. Derenzo, M. J. Weber, W. W. Moses, and C. Dujardin, IEEE Trans. Nucl. Sci. **47**, 860 (2000).
[7]T. Takizawa and C. Hidaka, J. Phys. Chem. Solids **69**, 347 (2008).
[8]A. J. J. Bos, R. M. van Duijvenvoorde, E. van der Kolk, W. Drozdowski, and P. Dorenbos, J. Lumin. **131**, 1465 (2011).
[9]E. van der Kolk, P. Dorenbos, J. T. M. de Haas, and C. W. E. van Eijk, Phys. Rev. B **71**, 045121 (2005).
[10]X. D. Yang, Z. Y. Xu, Z. Sun, B. Q. Sun, L. Ding, F. Z. Wang, and Z. Z. Ye., J. Appl. Phys. **99**, 046101 (2006).
[11]A. Bessiere, P. Dorenbos, C. W. E. van Eijk, E. Yamagishi, C. Hidaka, and T. Takizawa, J. Electrochem. Soc. **151**, H254 (2004).
[12]A. Anedda, C. M. Carbonaro, R. Corpino, M. Marceddu, O. B. Tagievc, and A. N. Georgobiani, J. Lumin. **128**, 1496 (2008).
[13]M. Ishikawa and T. Nakayama, Phys. Status Solidi C **4**, 823 (2004).